The stellar cusp around the Milky Way's central black hole

Rainer Schödel[1], Eulalia Gallego Cano[1], Francisco Nogueras Lara[1], Hui Dong[1], and Teresa Gallego Calvente[1]

[1] Instituto de Astrofísica de Andalucía (CSIC), Glorieta de la Astronomía s/n, 18008 Granada, Spain

Abstract

The existence of stellar cusps in dense clusters around massive black holes is a fundamental, decades-old prediction of theoretical stellar dynamics. Yet, observational evidence has been elusive so far. With a new, improved analysis of high-angular resolution images of the central parsecs of the Galactic Center, we are finally able to provide the first solid evidence for the existence of a stellar cusp around the Milky Way's massive black hole. The existence of stellar cusps is not only of theoretical importance, but has a significant impact on predicted event rates of phenomena like tidal disruptions of stars and extreme mass ratio inspiral events, which are expected to be strong sources of gravitational wave emission.

1 Introduction

Stellar clusters are not stationary objects, but evolve with time. For example, the destruction of a star near the centre of a cluster, or its ejection from the cluster, correspond to a loss of positive energy from the cluster, which will thus become more bound, i.e. contract. The stars in the cluster will then move faster, which means that a self-gravitating system has a negative heat capacity – it becomes hotter when energy is taken out. The presence of a massive black hole (MBH) in a cluster represents a special case that has been widely studied. If the MBH is not too massive, stars on certain trajectories will be destroyed once they approach the black hole to less than the tidal disruption radius. Close two-body encounters will lead to the randomisation of stellar orbits in the cluster over a so-called *relaxation time, t_r*. This process will repeatedly scatter stars onto orbits that will lead to their destruction near the MBH. If t_r is shorter than the age of the cluster, then a stellar cusp will form around the MBH. In that case the stellar number density will follow a power-law near the MBH, i.e. $\rho \propto r^{-\gamma}$, where ρ is the stellar density and r the distance from the black hole. This has been found by a large number of studies with different methods (Fokker-Planck approximations or n-body

simulations) under a wide range of initial conditions. For a cluster composed of single mass stars it has been found that $\gamma = 1.75$. In multi-mass clusters, the lightest stars will finally settle to a density distribution with $\gamma \approx 1.5$. Heavier components show steeper distributions. An overview of the theory on stellar cusps and ample references are given in [1].

Unfortunately, these predictions are not easy to test. On the one hand, galactic nuclei with massive black holes are too far from Earth so that we cannot resolve the individual stars. Measuring the light density can be misleading because it can be dominated by a small number of stars (see, eg., [18]). On the other hand, it is still not clear whether any globular clusters of the Milky Way contain an MBH (e.g., [16] vs. [21]).

Our best – and currently only – testbed for the theory of stellar cusps is therefore the Galactic Centre (GC). Located at a distance of 8.0 ± 0.25 kpc [15] It contains an MBH of about $4 \times 10^6 \, \mathrm{M_\odot}$ that is surrounded by a nuclear cluster of $2.5 \pm 0.4 \times 10^7 \, \mathrm{M_\odot}$ with a half-light radius of 4.2 ± 0.4 pc [11, 20, 4]. Since 1" corresponds to 0.039 pc at the distance of the GC and the angular resolution of adaptive optics (AO) assisted imaging at 8m-class telescopes at $2.2 \, \mu$m is about 0.06", we can thus resolve the nuclear cluster on scales of a few milli-parsecs.

Unfortunately, ambiguous results have been obtained by previous attempts to determine the presence and properties of a stellar cusp at the GC. For example, an analysis of the first near-infrared (NIR) AO assisted images from NACO/VLT came to the conclusion that there was a power-law cusp with $\gamma = 1.4 \pm 0.1$ [10], a value that was later revised downwards to $\gamma = 1.2 \pm 0.05$ [18]. These works did not take into account, however, that there is a significant number of young, massive stars present within a projected distance of $R < 0.5$ pc of Sagittarius A* (Sgr A*), the MBH [11]. With ages of just a few million years, the young stars cannot be dynamically relaxed and thus cannot serve as tracers of a potential stellar cusp. Subsequently, three studies excluded the young stars by spectroscopic or photometric criteria and examined only the distribution of bright giants (apparent magnitudes $K \lesssim 15.5$ at the GC). They came to the surprising conclusion that there was a core or possibly even a deficit of stars around Sgr A* [5, 7, 3].

There are numerous observational challenges to determining the stellar density distribution around Sgr A*, such as stellar crowding or variable extinction, but the most important one is probably the difficulty to classify the stars. On the one hand, the extreme extinction limits observational studies to the NIR, where intrinsic stellar colours are so small that reddening completely dominates the observed stellar colours. Spectroscopy, on the other hand, is limited to the brightest stars with seeing limited observations, or to intermediate bright stars ($K \lesssim 16$) with AO-assisted integral field spectroscopy, which works, moreover, only on very small fields because of instrumental limitations. Nevertheless, the observed stellar magnitudes (after correction for extinction) can provide a rough idea about the different types of stars. For the cusp-studies it is important to select tracer populations that can be old enough to be dynamically relaxed. At the GC, this corresponds to giants on the Red Clump (RC) ($K \lesssim 16$), or to faint (sub-)giants and main sequence stars ($K \gtrsim 18$). The RC stars dominate the number counts at bright magnitudes. They are 1-2 $\mathrm{M_\odot}$ He core burning stars, most of which are probably older than a few Gyr. With a two-body relaxation time at the GC of a few Gyr, they are adequate tracers for a potential cusp-like structure [1]. However, to resolve the ambiguity of previous studies, we must push toward fainter stars. For observed

magnitudes $K \approx 18$ and fainter, most stars will be of types potentially old enough to be dynamically relaxed (see, e.g., Fig. 16 in [18]). Previous studies were limited to brightness ranges $K \lesssim 17.5$. We therefore undertook a new study with the aim to push the detection limit toward fainter stars.

2   Data and methodology

We used NACO/VLT AO-assisted H and K_s imaging data obtained between 2010 and 2012. We selected data with excellent seeing and AO correction and short exposure times. The latter point is important because the detection of faint sources is rather limited by crowding than by sensitivity in the case of these data. Short exposure times avoid saturating the brightest stars and allowed us to estimate highly accurate PSFs, including their extended halos. We stacked the K_s images from four epochs, three in 2012 and one in 2011. Due to the relatively small time span, the high proper motion of stars in the GC, will only affect the PSFs of very few stars in the innermost arcsecond around Sgr A*. The variability of the PSF due to anisoplanatic effects was taken into account via analysing small fields with locally extracted PSFs, that were complemented by the seeing halo extracted from the brightest stars (similar to the methodology described in [19]).

The $H - K_s$ colours were used for extinction correction of individual stars and to create an extinction map that served to correct incompleteness due to extinction. The completeness due to crowding was determined with the technique of artificial stars. Source detection, astrometry, and photometry were performed with the program package *StarFinder* [6]. Uncertainties related to *StarFinder* performance were taken into account through repeated runs with different setting of the correlation threshold parameter, which dominates the probability of detecting sources (both real or spurious).

Star number counts are not the only source of information that we use. After subtracting all detected stars, we are left with the diffuse background light, which provides information on the stellar population that is too faint (and too crowded) to be detected as individual sources. A problem of the stellar diffuse emission is that it is so faint that it can be seriously contaminated by emission from the ionised gas in the GC mini-spiral. This can be clearly seen in the left hand panel of Fig. 1 that shows a point source-subtracted NACO Brackett-γ narrow band filter image, where the shape of the mini-spiral appears superposed onto the diffuse stellar background. Fortunately, the contribution of the ionised gas can be corrected by subtracting the suitably scaled Paschen-α emission that was mapped with the HST [8].

The Paα map is shown in the middle panel of Fig. 1 and the corrected Brγ map in the right panel. A few outliers remain in the image, which include remnant emission around IRS 7, the brightest source in the image, as well as emission from hot dust and ionised gas around compact extended sources, such as IRS 21 or IRS 1W, that are mostly bow-shocks [17]. Although the contribution from ionised gas is less important in broad-band filter images, it is still strong enough to cause a significant bias. Therefore we corrected all images of the diffuse emission with the help of the suitably scaled Paα emission map. We corrected the

resulting maps of the diffuse stellar light for differential extinction. In order to investigate systematics, we use maps from different filters (H, K_s, Brγ) and observing epochs.

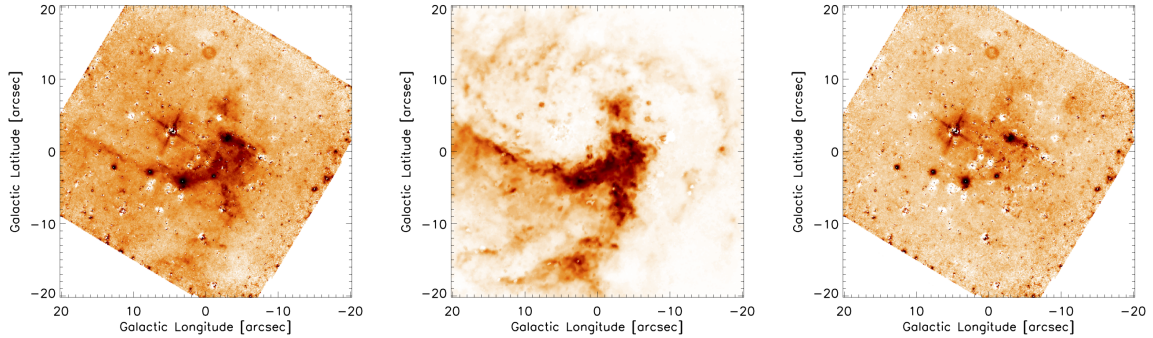Figure 1: Left: Point source-subtracted NACO/VLT image of the Brackett-γ emission at the GC. Middle: Point source-subtracted NIC3/HST image of the Paschen-α emission in the same region. Right: NACO Brγ image after subtraction of the suitably scaled HST Paα image.

3 Results

The obtained stellar number density and diffuse light density profiles are shown in Fig. 2. In the left panel we show, as a benchmark. the surface number density of bright to intermediate bright, spectroscopically identified old giants. This profile agrees, within the uncertainties, with previous findings [5, 7, 3]. An interesting point is that the interpretation of these data is ambiguous if we take a close look at them: If we exclude the data from the innermost arcsecond (0.04 pc), then the projected surface density can be fit by a simple power-law with an exponent $\Gamma = 0.4$. The previously cited papers obtained flatter power-laws for the central few 0.1 pc because they either were limited to studying only the central few arcseconds [7] or because they assumed broken-power laws, with steeper slopes beyond $\sim$0.5 pc [5]. It appears to be clear that there is a deficit of giants in the central $\sim$0.1 pc (in projection). Also, there seems to be a deficit around a projected radius $R \approx 0.2$ pc. But overall, there is no strong disagreement with the giants tracing a cusp.

The projected number density of the stars in the brightness range $17.5 \lesssim K_s \lesssim 18.5$ can be fit very well by a simple power law with $\Gamma = 0.4 \pm 0.04$. It is possible that some of the stars in this brightness range are not old stars. In fact, some contamination by pre-main sequence (MS) stars in the region $R \lesssim 0.5$ pc is probable because we know that there are young, massive stars present (see introduction). Unfortunately, we cannot yet directly identify these pre-MS stars. When we apply a rough correction, using the number densities and IMF derived for the young stars in this region [14], the projected power-law may flattens to values around $\Gamma \approx 0.2$. Nevertheless, the cusp does not disappear.
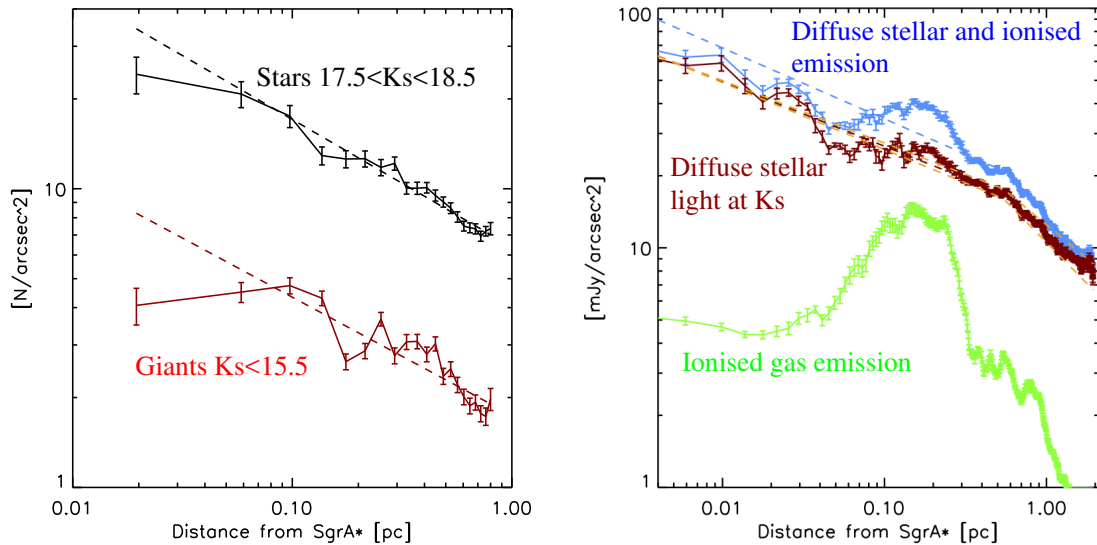
Figure 2: Left: The lower, red line shows the stellar number density for spectroscopically identified late-type (old) stars of $K_s \lesssim 15.5$. The dashed line is a simple power-law fit with an exponent of $\Gamma \approx 0.4$. The upper, black line shows the stellar number density for stars of $17.5 \lesssim K_s \lesssim 18.5$. The dashed line is a simple power-law fit with an exponent of $\Gamma \approx 0.4$. Right: Surface density of diffuse light from a point-source subtracted K_s NACO image. Blue: Total diffuse emission. HST Paα emission, tracing the ionised gas in the mini-spiral. Red: Diffuse light density after subtraction of contribution from ionised gas.

The right panel in Fig. 2 shows the profile of the projected diffuse stellar light in the K_s filter. A simple power-law with an exponent $\Gamma = 0.29 \pm 0.01$ provides an excellent fit to the data inside of $R \approx 0.5\,\mathrm{pc}$. Hence, in projection, there appears a power-law cusp in the stellar surface number densities and in the diffuse light from faint, unresolved stars. From simple assumptions about the stellar population in the GC, we estimate that the diffuse light is dominated by stars in the brightness range $K_s = 19 - 20$.

In conclusion, we detect a stellar cusp around Sgr A*. While there is some uncertainty with respect to the brightest giants, which may indeed show a deficit in the innermost $0.1 - 0.2\,\mathrm{pc}$, the fainter stars trace clear, simple power-laws. There may be some systematic pollution from young stars, in particular pre-MS stars. But this pollution would probably not make the cusp disappear in case of the $K_s \approx 18$ stars. Also, the fact that we observe very similar power-laws for three different tracer populations gives us confidence in the robustness of our result. We note that all three tracer populations, with mean brightnesses of $K_s \approx 15.5, 18.0, 19.5$ correspond to stars with mean ages of several Gyr and mean masses between $1 - 2\,\mathrm{M_\odot}$ (see, e.g., Fig. 16 in [18]). Hence, they all appear to be well-suited to inform us about the presence and properties of a stellar cusp.

In order to explore the intrinsic, three-dimensional structure of the nuclear star cluster,

we combined our NACO data of star counts and of the diffuse stellar light with measurements of the star and light densities at larger scales, from Spitzer [20] and HST/NACO/VVV [9]. Since the data at small and large scales were derived with different instruments, angular resolution, and filters, we first applied a scale factor to match them in their overlap regions. Then we subtracted a constant star/flux density in order to remove the contamination from other, overlapping components along the line of sight, e.g., the nuclear bulge or the Galactic Bar/Bulge. These components have scale lengths that are at least an order of magnitude greater than the size of the nuclear cluster (e.g., [13]). Therefore we can approximate their contribution very well by a constant offset. Subsequently, we fitted a three-dimensional Nuker-law [12] to the projected surface light density.
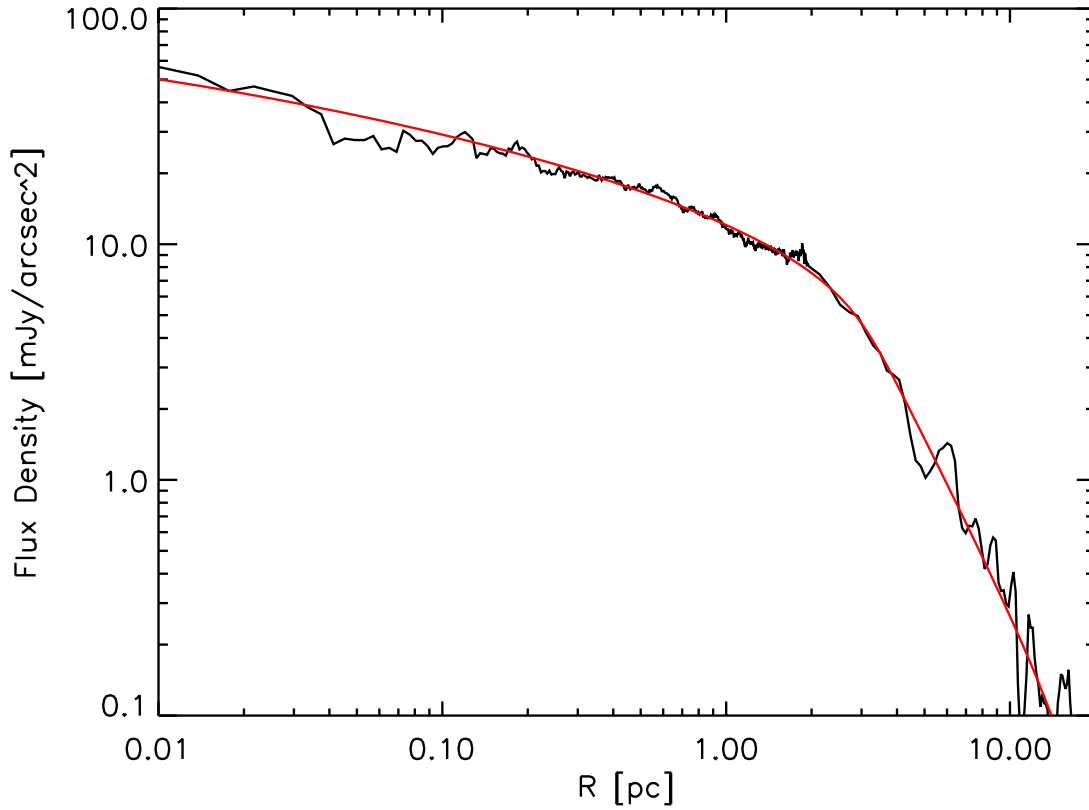

Figure 3: Nuker model fit (red line) to the diffuse surface brightness in the GC.

The 3D density distribution was defined as:

$$\rho(r) = \rho(r_b) 2^{(\beta-\gamma)/\alpha} \left(\frac{r}{r_b}\right)^{-\Gamma} \left[1 + \left(\frac{r}{r_b}\right)^{\alpha}\right]^{(\Gamma-\beta)/\alpha}, \tag{1}$$

Here, r is the 3D distance from Sgr A*, r_b is the break radius, ρ is the 3D density, γ is the

exponent of the inner and β the one of the outer power-law, and α defines the sharpness of the transition. The density was then projected along the line of sight via an integral:

$$\Sigma(R) = 2 \int_R^\infty \frac{r\rho(r)dr}{\sqrt{r^2 - R^2}} \tag{2}$$

In order to determine the uncertainties, we varied several of our initial assumptions, e.g., the value of the subtracted constant offset, the value of the parameter α, or the integration boundaries along the line-of-sight. For the diffuse light, we obtain the following best-fit parameters:$r_b = 3.31 \pm 0.31\,\mathrm{pc}$, $\gamma = 1.16 \pm 0.02$, $\beta = 3.26 \pm 0.39$, and $\rho(r_b) = 059 \pm 0.10\,\mathrm{mJy\,pc^{-3}}$. The data, along with the best fit, are shown in Fig. 3. Fits to the different tracers of the observed stellar number density (RC and faint subgiants) result in similar numbers, but slightly higher values of $\gamma \approx 1.3$. This can reflect, on the one hand, the true uncertainty range of our study. On the other hand, the stellar number surface density is probably contaminated by the presence of young (pre-)mainsequence stars in the innermost few 0.1 pc (see, e.g., [3, 14]). We estimated the contribution of these contaminants with the result that when we take them into account the value of γ decreases to $\gamma \approx 1.2$.

4   Discussion and conclusion

Our analysis of the stellar number density and of the diffuse stellar light density around the MBH at the centre of the Milky Way has revealed that the density distribution follows a power-law with an exponent of $\gamma \approx 1.2$, in three dimensions. This power-law is valid from the immediate vicinity of Sgr A* to a distance of about 2 pc. Beyond a break radius of roughly 3 pc, the power-law steepens considerably and the density falls off rapidly toward the edge of the nuclear star cluster. The cusp is therefore well developed inside the radius of influence of the MBH, which is about 3 pc [1, 20]. We can rule out a flat core with extremely high significance.

Surprisingly, the stellar cusp at the centre of the Milky Way is significantly flatter than predicted by most previous theoretical work, which led us to expect $\gamma_{\mathrm{theor}} \approx 1.5$ for stars in the mass range investigated by us (see introduction and discussions in, e.g., [1, 18]). A plausible explanation for this discrepancy is that most theoretical work focused on idealised systems, for example, fully relaxed clusters with single-age stellar populations. New n-body numerical models carried out in parallel to our observational work produce a stellar cusp with very similar properties as observed by us. The new work (Baumgardt, Amaro-Seoane & Schödel, in prep.) includes repeated episodes of star formation – in a quasi-continuous way – into the dynamical development of the nuclear cluster. As a consequence, the younger stellar populations had less time to relax dynamically, which flattens the cusp.

To conclude, we believe that we have found robust evidence for a stellar cusp at the GC. For the first time, theory and observations have converged on the question of the stellar cusp. This does not only provide a test of the validity of the fundaments of theoretical stellar dynamics. A further implication of our work is that stellar cusps exist probably around many other MBHs in the Universe. This is an important pre-requisite for so-called Extreme Mass Ratio Inspirals (EMRIs) to occur frequently enough to be observable with future gravitational

wave observatories in space, such as eLISA. In an EMRI, a compact, low mass object, such as a neutron star or a stellar mass black hole, spiral into an MBH. The associated burst of gravitational wave emission is an exquisite probe of the properties of the MBH and of General Relativity (see, e.g., [2]).

The results underlying this article will soon be submitted in the form of various articles to A&A (Gallego-Cano et al., Schödel et al.; Baumgardt, Amaro-Seaone & Schödel).

Acknowledgments

References

[1] Alexander, T. 2005, Physics Reports, 419, 65

[2] Amaro-Seoane, P., Gair, J. R., Freitag, M. et al. 2007, Classical and Quantum Gravity, 24, 113

[3] Bartko, H., Martins, F., Trippe, S. et al. 2010, ApJ, 708, 834

[4] Boehle, A., Ghez, A. M., Schödel, R. et al. 2016, ApJ, 830, article id.17

[5] Buchholz, R., Schödel, R. & Eckart, A. 2009, A&A, 499, 483

[6] Diolaiti, E., Bendinelli, O., Bonaccini, D. et al. 2000, A&AS, 147, 335

[7] Do, T., Ghez, A. M., Morris, M. R. et al. 2009, ApJ, 704, 1323

[8] Dong, H., Wang, D., Cotera, A. et al. 2011, MNRAS, 417, 114

[9] Fritz, T., Chatzopoulos, S., Gerhard, O. et al. 2016, ApJ, 821, 44

[10] Genzel, R., Schödel, R., Ott, T. et al. 2003, ApJ, 594, 812

[11] Genzel, R., Eisenhauer, F. & Gillessen, S. 2010, Rev. Mod. Phys., 82, 3121

[12] Lauer, T. R., Ajhar, E. A., Dressler, A. et al. 1995, AJ, 110, 2622

[13] Launhardt, R., Zylka, R. & Mezger, P. G. 2002, A&A, 384, 112

[14] Lu, J. r., Do, T., Ghez, A. M. et al. 2013, ApJ, 764, 155

[15] Malkin, Z. 2013, Proceedings IAU Symposium No. 289, Richard de Grijs, ed., 289, 406

[16] Noyola, E., Gebhardt, K., et al. 2010, ApJL, 719, L60

[17] Sánchez-Bermúdez, J., Schödel, R., Alberdi, A. et al. 2014, A&A, 567, A21

[18] Schödel, R., Eckart, A., Alexander, T. et al. 2007, A&A, 469, 125

[19] Schödel, R. 2010, A&A, 509, A58

[20] Schödel, R., Feldmeier, A., Kunneriath, D. et al. 2014, A&A, 566, A47

[21] van der Marel, R. P. & Anderson, J. 2010, ApJ, 710, 1063